Available online at www.sciencedirect.com

ScienceDirect

Energy Procedia 158 (2019) 6576–6581

Energy Procedia

www.elsevier.com/locate/procedia

10th International Conference on Applied Energy (ICAE2018), 22-25 August 2018, Hong Kong, China

Extended MANA Formulation for Time-domain Simulations of Combined Power and Gas Networks

Xiaopeng Fu[a]*, Peng Li[a], Chengshan Wang[a], Jean Mahseredjian[b]

[a]*Tianjin University, 92 Weijin Road, Tianjin 300072, China*
[b]*Polytechnique Montréal, C.P. 6079 succ. Centre-ville, Montréal H3C 3A7, Canada*

Abstract

The promise of improved system efficiency, reliability, and higher renewable energy hosting capability of the Integrated Energy System concept has driven the development of innovative network coupling technologies and energy system integration methods. Co-ordinated design and operation of the traditionally separate energy systems, including electric power, gas, and heat will lead to the optimal use of synergies between energy networks and bring forth numerous benefits to the energy sector. To fully understand the potential and quantitatively assess the operation performance of the combined energy networks, a unified modeling and simulation framework using an extended MANA formulation is proposed in this paper, which is capable of incorporating arbitrary gas network configurations and unbalanced power networks in a systematic manner needed. A case study with combined power and gas networks via EnergyHubs is implemented to demonstrate the application of the proposed method.

© 2019 The Authors. Published by Elsevier Ltd.
This is an open access article under the CC BY-NC-ND license (http://creativecommons.org/licenses/by-nc-nd/4.0/)
Peer-review under responsibility of the scientific committee of ICAE2018 – The 10th International Conference on Applied Energy.

Keywords: Dynamic simulation; time-domain simulation; combined power and gas networks; integrated energy systems

1. Introduction

The energy systems are experiencing important transitions due to the increasing penetration of renewable energy sources, greenhouse gas emission targets, and higher demands of energy supply reliability. One significant aspect of this transition is the increasing coupling and interactions among multiple energy networks, e.g. electric power, gas,

* Corresponding author. Tel.: +86-158-2288-8351.
E-mail address: fuxiaopeng@tju.edu.cn

1876-6102 © 2019 The Authors. Published by Elsevier Ltd.
This is an open access article under the CC BY-NC-ND license (http://creativecommons.org/licenses/by-nc-nd/4.0/)
Peer-review under responsibility of the scientific committee of ICAE2018 – The 10th International Conference on Applied Energy.
10.1016/j.egypro.2019.01.072

and heat networks, especially in their distribution networks, where the coupling is prominent due to innovative technologies, including the Combined Heat and Power units (CHP), Power to Gas equipment (P2G), fuel cells, etc. In theory, the different and possibly complementary spatial and temporal characteristics of these energy networks could lead to improved system efficiency and reliability, through coordinated operation of multiple energy networks using an Integrated Energy System (IES) approach [1]. However, to fully understand and realize the potential of this IES approach, and quantitatively assess the operation performance of the combined energy networks, a unified modeling and simulation framework is urgently needed.

The EnergyHub model, initially proposed in [2] and later enhanced, e.g. in [3], provides a standardized formulation for the steady-state power conversion relationship between different energy forms of a group of network coupling equipment. Integrated steady-state analysis formulation incorporating electric power, gas, and heat networks is proposed in [4] and [5] based on the Newton-Raphson solution approach. On the other hand, a well-established framework for the dynamic simulation of the combined multiple energy networks is still lacking. In [6] and [7], the gas pipeline networks are modeled using block diagrams in the MATLAB/Simulink platform, using a fixed spatially discretized model from the original governing PDEs for gas networks. Besides being rigid on the solution algorithm and not scalable for practical large systems, this approach is unable to exploit the timescale property of the combined networks. In [8], a quasi-dynamic approach named SAInt is utilized for the combined power and gas transmission networks, where the steady-state model of power networks is coupled with the dynamic model of gas networks, assuming the time constants of the former is significantly smaller than that of the latter. It is further assumed that the power networks operate in the optimal condition at each time step. This approach is inappropriate when the focus is on the energy distribution networks, e.g. community IES, as the power distribution networks are unbalanced and the positive sequence-based power flow equations are not sufficient. It is also better to model the EMS control actions separately to reflect the complexity of power system operations.

In this paper, we utilize the Modified Augmented Nodal Analysis (MANA) formulation, which is well-established for both steady-state and time-domain analysis in power system simulations, e.g. in EMTP [9], and extend it to incorporate gas network components in a systematic manner. The proposed formulation is versatile and capable of modeling unbalanced power networks, arbitrary gas pipeline configurations, and other gas network facilities such as compressor and regulator stations, allowing unified time-domain simulation of combined multiple energy networks with easy extendibility.

2. MANA formulation for power networks

MANA formulation of power networks is achieved by augmenting the classical nodal equations with supplementary component equations. A generic form of the network equation can be written as:

$$\begin{bmatrix} \mathbf{Y}_\mathrm{n} & \mathbf{A}_\mathrm{c} \\ \mathbf{A}_\mathrm{r} & \mathbf{A}_\mathrm{d} \end{bmatrix} \begin{bmatrix} \mathbf{v}_\mathrm{n} \\ \mathbf{i}_\mathrm{x} \end{bmatrix} = \begin{bmatrix} \mathbf{i}_\mathrm{n} \\ \mathbf{v}_\mathrm{x} \end{bmatrix} \tag{1}$$

where $\mathbf{Y}_\mathrm{n}$ is the classical nodal admittance matrix, $\mathbf{v}_\mathrm{n}$ and $\mathbf{i}_\mathrm{x}$ are node voltages and component currents, $\mathbf{i}_\mathrm{n}$ and $\mathbf{v}_\mathrm{x}$ are known nodal currents and component voltages, respectively. The augmented $\mathbf{A}_\mathrm{c}$, $\mathbf{A}_\mathrm{r}$, $\mathbf{A}_\mathrm{d}$ matrices enable representing the component model contributions that are not easily included in $\mathbf{Y}_\mathrm{n}$, which will be illustrated in section 2.2.

2.1. MANA formulation for steady-state and time-domain analysis

The MANA formulation is a unified framework for both steady-state and time-domain analysis, where each component of power networks is associated with unique model stamps and contributes a portion to the MANA formulation matrix and vector in a systematic manner.

In the time-domain analysis, component models are discretized using implicit integration formulas and transformed into Norton equivalent circuit composed of an equivalent conductance G_eq and a history current source I_h. The equivalent conductance contributes to the $\mathbf{Y}_\mathrm{n}$ matrices and the history current source contributes to the $\mathbf{i}_\mathrm{n}$ vector in the MANA formulation.

In the steady-state analysis, phasor models are used for power network components. This represents a different set of model stamps and the MANA formulation equation is in complex numbers.

An example illustrating the MANA formulation for both steady-state and time-domain simulation is shown in Fig. 1. The steady-state equations are:

$$\begin{bmatrix} \frac{1}{j\omega L_1}+j\omega C_1+\frac{1}{R_1} & -\frac{1}{R_1} & 0 & -\frac{1}{j\omega L_1} & 0 \\ -\frac{1}{R_1} & \frac{1}{R_1}+\frac{1}{j\omega L_2} & -\frac{1}{j\omega L_2} & 0 & 0 \\ 0 & -\frac{1}{j\omega L_2} & \frac{1}{j\omega L_2}+j\omega C_2 & 0 & 0 \\ -\frac{1}{j\omega L_1} & 0 & 0 & \frac{1}{j\omega L_1} & 1 \\ 0 & 0 & 0 & 1 & 0 \end{bmatrix} \begin{bmatrix} V_1 \\ V_2 \\ V_3 \\ V_4 \\ I_{v_s} \end{bmatrix} = \begin{bmatrix} 0 \\ 0 \\ 0 \\ 0 \\ V_s \end{bmatrix}$$

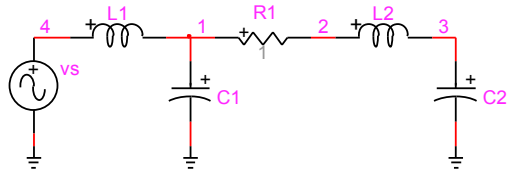

Fig. 1. Illustrating example for MANA formulation for both steady -state and time-domain analysis.

whereas the time-domain equations are:

$$\begin{bmatrix} \Delta t/2L_1+2C_1/\Delta t+1/R_1 & -1/R_1 & 0 & -\Delta t/2L_1 & 0 \\ -1/R_1 & 1/R_1+\Delta t/2L_2 & -\Delta t/2L_2 & 0 & 0 \\ 0 & -\Delta t/2L_2 & \Delta t/2L_2+2C_2/\Delta t & 0 & 0 \\ -\Delta t/2L_1 & 0 & 0 & \Delta t/2L_1 & 1 \\ 0 & 0 & 0 & 1 & 0 \end{bmatrix} \begin{bmatrix} v_1 \\ v_2 \\ v_3 \\ v_4 \\ i_{v_s} \end{bmatrix} = \begin{bmatrix} i_{L_1h}-i_{C_1h} \\ -i_{L_2h} \\ i_{L_2h}-i_{C_2h} \\ -i_{L_1h} \\ v_s \end{bmatrix}$$

2.2. MANA formulation for multiphase power flow analysis

The flexibility of the MANA formulation enables it to incorporate component constraint equations that are difficult for other formulation method. Moreover, it is shown in [10] that the power flow constraints can be included in the aforementioned steady-state MANA formulation and achieves a multiphase power flow analysis. The generic form for the load flow MANA formulation is

$$\begin{bmatrix} \mathbf{A}_{\mathrm{N}}^{\mathrm{LF}} & \mathbf{A}_{\mathrm{I}} \\ \mathbf{L}_{\mathrm{LA}} & \mathbf{L}_{\mathrm{d}} \end{bmatrix} \begin{bmatrix} \Delta\mathbf{x} \\ \Delta\mathbf{x}_{\mathrm{LF}} \end{bmatrix} = -\mathbf{f}_{\mathrm{LF}} \tag{2}$$

where $\mathbf{A}_{\mathrm{N}}^{\mathrm{LF}}$ is the real version of the original complex matrix from the steady-state analysis MANA equation in (1), $\mathbf{A}_{\mathrm{I}}$ is a connectivity matrix for the load-flow devices, $\mathbf{L}_{\mathrm{LA}}$ and $\mathbf{L}_{\mathrm{d}}$ are coefficient matrices for the load-flow constraint equations.

The construction of the matrices in (2) is illustrated by considering a single-phase PQ load, labeled as the pth load flow device and connected between node k and m. The load flow constraint equations are:

$$P_p - V_{km}^R I_p^R - V_{km}^I I_p^I = f_{L_p}^R = 0, \quad Q_p - V_{km}^I I_p^R + V_{km}^R I_p^I = f_{L_p}^I = 0 \tag{3}$$

The contribution of this device to the load flow Jacobian matrix is thus

$$\begin{bmatrix} -I_p^{R(l)} & -I_p^{I(l)} \\ I_p^{I(l)} & -I_p^{R(l)} \end{bmatrix} \begin{bmatrix} \Delta V_{km}^R \\ \Delta V_{km}^I \end{bmatrix} + \begin{bmatrix} -V_{km}^{R(l)} & -V_{km}^{I(l)} \\ -V_{km}^{I(l)} & V_{km}^{R(l)} \end{bmatrix} \begin{bmatrix} \Delta I_p^R \\ \Delta I_p^I \end{bmatrix} = \begin{bmatrix} -f_{L_p}^{R(l)} \\ -f_{L_p}^{I(l)} \end{bmatrix} \tag{4}$$

where the superscript l represents the lth iteration. The two coefficient matrices in (4) contribute to $\mathbf{L}_{\mathrm{LA}}$ and $\mathbf{L}_{\mathrm{d}}$ in (2), respectively. A complete discussion of different power flow constraint equations is referred to [10].

3. Extended MANA formulation for gas networks

In this section, we first present mathematical models of various gas network branch and node models, including gas pipelines, compressor and regulator stations, source and loads. We then show that these model equations can be systematically included into an extended MANA formulation (5) to achieve unified modeling.

$$\begin{bmatrix} \mathbf{A}_{\mathrm{e}} & \mathbf{A}_{\mathrm{cp1}} \\ \mathbf{A}_{\mathrm{cp2}} & \mathbf{A}_{\mathrm{g}} \end{bmatrix} \begin{bmatrix} \mathbf{x}_{\mathrm{e}} \\ \mathbf{x}_{\mathrm{g}} \end{bmatrix} = \begin{bmatrix} \mathbf{b}_{\mathrm{e}} \\ \mathbf{b}_{\mathrm{g}} \end{bmatrix} \tag{5}$$

In Eq. (5), $\mathbf{A}_{\mathrm{e}}$, $\mathbf{x}_{\mathrm{e}}$ and $\mathbf{b}_{\mathrm{e}}$ are the MANA formulation matrix and vectors in (1) for the power networks. We use the power flow analysis formulation in this paper as the time constants of the power networks are considerably small compared to the timescale of this research; however, dynamical formulation for the power networks are readily available if faster transients in the combined network is of interest. Matrices $\mathbf{A}_{\mathrm{cp1}}$ and $\mathbf{A}_{\mathrm{cp2}}$ represents the coupling factor from gas to power and power to gas, respectively. These factors arise due to components such as gas turbine generators, which couple the gas network loads to the power network generations. $\mathbf{A}_{\mathrm{g}}$, $\mathbf{b}_{\mathrm{g}}$ represents gas network topology and boundary conditions and are explained more explicitly in the following; $\mathbf{x}_{\mathrm{g}}$ is the gas network variable.

3.1. Gas networks: pipeline equations

The governing equations for the gas pipelines under the one-dimensional isothermal flow assumption are well documented in [6]-[8], which include the continuity equation (6) and the momentum equation (7):

$$\frac{A}{c^2}\frac{\partial p}{\partial t}+\frac{\partial M}{\partial x}=0 \tag{6}$$

$$\frac{\partial p}{\partial x}+\frac{1}{A}\frac{\partial M}{\partial t}+\frac{\lambda c^2 M|M|}{2DA^2 p}=0 \tag{7}$$

where p is the gas pressure, c is the isothermal speed of sound, M is the mass flow rate, A is the cross-section area, λ is the friction factor. Notice that in contrast to power networks, the gas network model is a set of partial differential equations (PDEs).

For a short pipeline connected between node k and m, the following discretization formula is used in this paper:

$$\begin{cases}\frac{A}{c^2}\frac{p_m(t_{n+1})-p_m(t_n)}{\Delta t}+\frac{M_m(t_{n+1})-M_k(t_{n+1})}{\Delta x}=0\\ \frac{p_m(t_{n+1})-p_k(t_{n+1})}{\Delta x}+\frac{1}{A}\frac{M_k(t_{n+1})-M_k(t_n)}{\Delta t}+\frac{\lambda c^2 M_k(t_{n+1})|M_k(t_n)|}{2DA^2 p_m(t_n)}=0\end{cases} \tag{8}$$

In order to develop model stamps for the gas network components in the MANA formulation, the lower part of Eq. (5), for a gas network with N nodes and L branches, is written more explicitly as

$$\mathbf{A}_{\mathrm{cp2}}\mathbf{x}_{\mathrm{e}}+\begin{bmatrix}\mathbf{A}_{\mathbf{cp}} & \mathbf{A}_{\mathrm{c}\mathbf{M}} & \mathbf{A}_{\mathbf{cr}}\\ \mathbf{A}_{\mathrm{m}\mathbf{p}} & \mathbf{A}_{\mathrm{m}\mathbf{M}} & \mathbf{A}_{\mathrm{m}\mathbf{r}}\\ \mathbf{A}_{\mathrm{n}\mathbf{p}} & \mathbf{A}_{\mathrm{n}\mathbf{M}} & \mathbf{A}_{\mathrm{n}\mathbf{r}}\\ \mathbf{A}_{\mathbf{dp}} & \mathbf{A}_{\mathrm{d}\mathbf{M}} & \mathbf{A}_{\mathbf{dr}}\end{bmatrix}\begin{bmatrix}\mathbf{p}\\ \mathbf{M}\\ \mathbf{r}\end{bmatrix}=\begin{bmatrix}\mathbf{b}_{\mathrm{g1}}\\ \mathbf{b}_{\mathrm{g2}}\\ \mathbf{b}_{\mathrm{g3}}\\ \mathbf{b}_{\mathrm{g4}}\end{bmatrix} \tag{9}$$

where $\mathbf{p}\in\mathcal{R}^N$ is the node pressure vector, $\mathbf{M}=[\mathbf{M}_{\mathrm{k}};\ \mathbf{M}_{\mathrm{m}}]\in\mathcal{R}^{2L}$ is the mass flow rate vector, with $\mathbf{M}_{\mathrm{k}}, \mathbf{M}_{\mathrm{m}}\in\mathcal{R}^L$ represents the flow rates at the from node and to node, respectively; $\mathbf{r}$ represents additional device variables. Submatrices with first subscript being c and m have L rows; those with first subscript n have N rows, and the row number of those with first subscript d is dependent on the property of the non-pipe branches.

From Eqs. (8), it is observed that pipeline models with the proposed discretization contribute only to the $\mathbf{A}_{\mathbf{cp}}$, $\mathbf{A}_{\mathrm{c}\mathbf{M}}$, $\mathbf{A}_{\mathrm{m}\mathbf{p}}$, $\mathbf{A}_{\mathrm{m}\mathbf{M}}$ matrices. For a pipeline which is labeled as branch p and connected between node k and m, the model stamp is shown in Fig. 2(a).

3.2. Gas networks: other branch equations

The compressor and regulator stations are used as example to explain the formulation of other non-pipe branch models. The gas flow rate entering and exiting the station remains unchanged, i.e.

$$M_k=M_m \tag{10}$$

The node pressure at two terminals of the station is related by

$$p_m = \begin{cases} r_{\max} p_k & if\ r > r_{\max} \\ r p_k & if\ r_{\min} < r < r_{\max} \\ r_{\min} p_k & if\ r < r_{\min} \end{cases} \tag{11}$$

Eqs. (10) and (11) establish relationships between the vector **p** and **M**, and enters the first and second row in (9). The compressor/regulator station model also maintains an additional state variable with:

$$\frac{d}{dt} r = \frac{1}{T}(p_{\text{ref}} - p_m) \tag{12}$$

Eq. (12) is discretized with implicit integration method and the resulting equation enters the last row in Eq. (9).

For a compressor or regulator station labeled as branch p and connected between node k and m, which also maintains the lth device state variable, the model stamp is illustrated in Fig. 2(b).

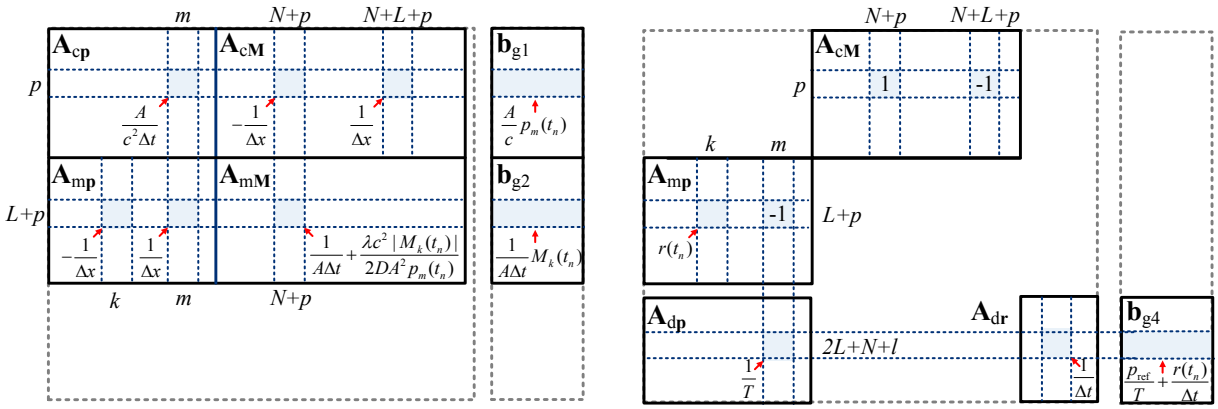

(a) gas pipeline (b) compressor & regulator station

Fig. 2. MANA formulation model stamps for (a) gas pipeline, and (b) compressor and regulator station.

3.3. Gas networks: node constraint equations

In each node of the gas network, the sum of the inbound gas flow rate from connected pipelines, gas sources, etc. should equal to the sum of outbound gas flow rate from connected pipelines, loads, etc. These equations enter the third row of Eq. (9), where the source stations and gas loads contribute to $\mathbf{b}_{g3}$.

4. Case studies

A case study is carried out to test and validate the proposed extended MANA formulation. The test case, as shown in Fig. 3, is consist of the IEEE 13 node test feeder system, coupled with a four-node gas distribution network with a compressor station. The power network parameters are referred to [11], and the gas network parameters are labeled in Fig. 3. The coupling of the two networks is via two EnergyHubs, which binds Bus#8 in the power network with Bus#3 in the gas network, and Bus#14 in the power network with Bus#4 in the gas network, respectively. The electric and thermal loading of the two EnergyHubs in a typical day is displayed in Fig. 4. Two conventional operating modes of the EnergyHubs that include CHP units are thermal load following (FTL) and electric load following (FEL). In this case study, both operation modes are tested in a period of 24 hours with the proposed time-domain simulation formulation. Electric loads on other power network buses are assumed to vary uniformly with the same pattern of the average of the electrical loads of the two EnergyHubs.

The simulation results are presented in Fig. 5, where the simulation curves of the gas flow rate and the node pressure at the output terminal of pipeline P1 are compared under the two different operation modes of the EnergyHubs. It is observed that the variation of the node pressure is larger under the FEL mode, as the heavier electric load requires the CHP units in the EnergyHubs to consume more fuels. Correspondingly, the voltage profile of the distribution network is better, especially for EB14 at the end of the feeder. Due to space limit, power network results are not displayed.

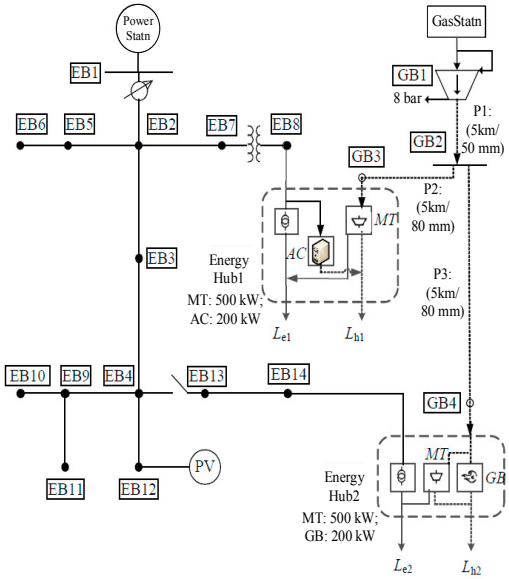

Fig. 3. Combined gas and power networks test case.

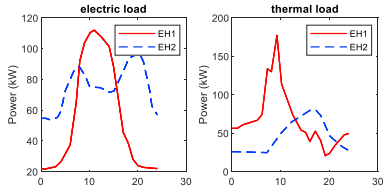

Fig. 4. Loading profile of EnergyHubs.

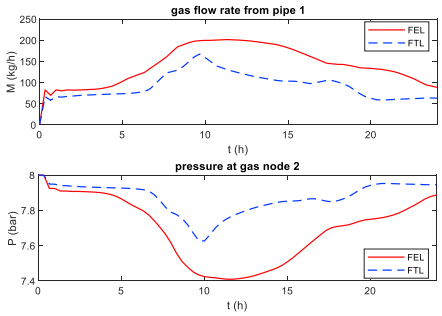

Fig. 5. Test case time-domain simulation results.

5. Conclusion

This paper proposes an extended MANA formulation for the time-domain simulation of the combined power and gas networks. The flexibility of the MANA formulation is first demonstrated through unified modeling for both power-flow and time-domain analysis of power networks. A systematic approach is then developed for incorporating gas network component and constraint equations into the MANA equations. A test case of coupled unbalanced power network and gas distribution network was simulated to test and validate the proposed extended MANA formulation.

Acknowledgements

This research was supported by National Natural Science Foundation of China (No. 51807131).

References

[1] Liu X, Mancarella P. Modelling, assessment and Sankey diagrams of integrated electricity-heat-gas networks in multi-vector district energy systems. Applied Energy, 2016: 336-352.
[2] Geidl M, Koeppel G, Favreperrod P, et al. Energy hubs for the future. IEEE Power & Energy Magazine, 2007, 5(1): 24-30.
[3] Wang Y, Zhang N, Kang C, et al., Standardized matrix modeling of multiple energy systems. IEEE Transactions on Smart Grid, early access.
[4] Martinezmares A, Fuerteesquivel C R. A unified gas and power flow analysis in natural gas and electricity coupled networks. IEEE Transactions on Power Systems, 2012, 27(4): 2156-2166.
[5] Abeysekera M and Wu J. Method for simultaneous power flow analysis in coupled multi-vector energy networks. Energy Procedia, 2015, 75, pp. 1165-1171.
[6] Behbahaninejad M, Bagheri A. The accuracy and efficiency of a MATLAB-Simulink library for transient flow simulation of gas pipelines and networks. Journal of Petroleum Science and Engineering, 2010, 20: 256-265.
[7] Xu X, Jia H, Chiang HD, Yu DC, Wang D. Dynamic modeling and interaction of hybrid natural gas and electricity supply system in microgrid. IEEE Transactions on Power Systems. 2015;30(3):1212-1221.
[8] Pambour K A, Erdener B C, Boladolavin R, et al. SAInt – A novel quasi-dynamic model for assessing security of supply in coupled gas and electricity transmission networks. Applied Energy, 2017: 829-857.
[9] Mahseredjian J, Dennetiere S, Dube L, et al. On a new approach for the simulation of transients in power systems. Electric Power Systems Research, 2007, 77(11): 1514-1520.
[10] Kocar I, Mahseredjian J, Karaagac U, et al. Multiphase load-flow solution for large-scale distribution systems using MANA. IEEE Transactions on Power Delivery, 2014, 29(2): 908-915.
[11] Kersting W H. Radial distribution test feeders. IEEE Transactions on Power Systems, 1991, 6(3): 975-985.